*BALADI & ROHANI

A TERRAIN-VEHICLE MODEL FOR ANALYSIS OF STEERABILITY OF TRACKED VEHICLES

GEORGE Y. BALADI, PH.D.
BEHZAD ROHANI, PH.D.
U.S. ARMY ENGINEER WATERWAYS EXPERIMENT STATION
VICKSBURG, MISSISSIPPI 39180

INTRODUCTION

Development of high-mobility/agility tracked combat vehicles has received considerable attention recently because of the possibilities they offer for increased battlefield survivability through the avoidance, by high-speed and violent maneuver, of hits by high-velocity projectiles and missiles. In order to design and develop such vehicles rationally, it is necessary to have a quantitative understanding of the interrelationship between the terrain factors (such as soil type, soil shear strength and compressibility, etc.) and the vehicle's characteristics (weight, track length and width, location of center of gravity, velocity, etc.) during steering. To study such an interrelationship, it is necessary to construct idealized mathematical models of the terrain-vehicle interaction. The accuracy and range of application of such models must, of course, be determined from actual mobility experiments, and obviously must depend on the degree of relevance of the idealized model as an approximation to the real behavior.

The basic concepts of the theory of terrain-vehicle interaction were developed by Bekker during the 1950's (1). By assuming various load distributions along the tracks, Bekker was able to develop several mathematical expressions relating the characteristics of the vehicle and the tractive effort of the terrain during steering. By considering the lateral and longitudinal coefficients of friction between the track and the ground, Hayashi (2) developed simple equations for practical analysis of steering of tracked vehicles. Hayashi's work, however, did not include the effect of the centrifugal forces on steering performance of the vehicle. Kitano and Jyorzaki (3)

developed a more comprehensive model for uniform turning motion including the effects of centrifugal forces. This model, however, is based on the assumption that ground pressure is concentrated under each road wheel and the terrain-track interaction is simulated by Coulomb-type friction. The model given in Kitano and Jyorzaki was extended by Kitano and Kuma (4) to include nonuniform (transient) motion, but the basic elements of the terrain-track interaction part of the model were retained. Baladi and Rohani (5) developed a model for uniform turning motion parallel to the development reported in Reference 3 insofar as the kinematics of the vehicle are concerned. In contrast to Reference 3, however, this model is based on a more comprehensive soil model. In the present paper, the terrain-vehicle model reported in Reference 5 is extended to include nonuniform (transient) motion. In addition, the soil model is modified to include a nonlinear failure envelope describing the shearing strength of the terrain material.

To demonstrate the application of the model, the steering performance of an armored personnel carrier has been predicted and correlated with full-scale test results.

SOIL MODEL

Strength Components

One of the most important properties of soil affecting trafficability is the in situ shear strength of the soil. The shear strength of earth materials varies greatly for different types of soil and is dependent on the confining pressure and time rate of loading (shearing). This dependence, however, is not the same for all soils and varies with respect to two fundamental strength properties of soil: the cohesive and the frictional properties. It has been found experimentally that the shear strength of purely cohesive soils (soils without frictional strength) is independent of the confining stress and is strongly affected by the time rate of shearing. On the other hand, in the case of purely frictional soil (soils without cohesive strength), the shear strength is found to be independent of time rate of loading and is strongly dependent on the confining pressure. In nature, most soils exhibit shearing resistance due to both the frictional and cohesive components. The cohesive and frictional components of strength are usually added together in order to obtain the total shear strength of the material, i.e.,

$$\tau_M = A - M \exp(-N\sigma) \qquad (1)$$

where τ_M is the maximum shearing strength of the material,

(164)

C = A - M is the cohesive strength of the material corresponding to static loading (very slow rate of deformation), σ is normal stress, and N is a material constant. Equation 1 is shown graphically in Figure 1.

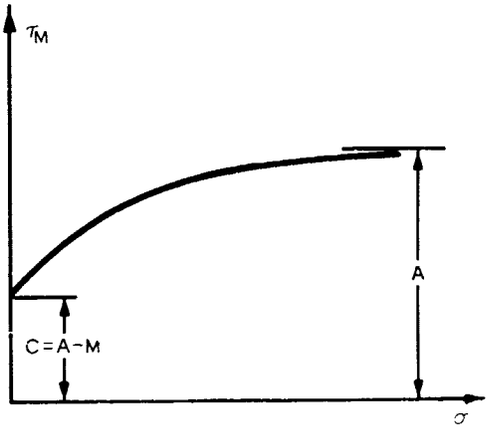

Figure 1. Proposed failure relation for soil.

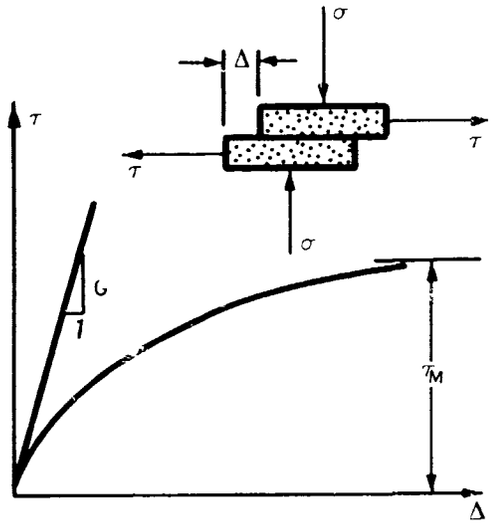

Figure 2. Proposed soil-stress/deformation relation during shearing process.

Effect of Rate of Deformation

As was pointed out previously, the cohesive strength of the material is dependent on the time rate of loading (shearing); i.e., the cohesive component of strength increases with increasing rate of loading. For the range of loading rates associated with the motion of tracked vehicles, the contribution to cohesive strength due to dynamic loading can be expressed as $C_d\left[1 - \exp(-\Lambda\dot{\Delta})\right]$, where C_d and Λ are material constants, and $\dot{\Delta}$ is time rate of shearing deformation. In view of the above expression and Equation 1, the dynamic failure criterion takes the following form:

$$\tau_M = A + C_d\left[1 - \exp(-\Lambda\dot{\Delta})\right] - M\exp(-N\sigma) \qquad (2)$$

Shear Stress-Shear Deformation Relation

Prior to failure, the shear stress-shear deformation characteristics of a variety of soils can be expressed by the following mathematical expression (6):

(165)

$$\tau = \frac{G\,\tau_M\,\Delta}{\tau_M + G|\Delta|} \tag{3}$$

The behavior of Equation 3 is shown graphically in Figure 2. In Figure 2, τ denotes shearing stress, Δ is shearing deformation, and G is the initial shear stiffness coefficient. In view of Equation 2, the shear stress-shear deformation relation for soil (Equation 3) becomes

$$\tau = \frac{G\left[A + C_d - C_d \exp(-\lambda\dot{\Delta}) - M \exp(-N\sigma)\right]\Delta}{G|\Delta| + A + C_d - C_d \exp(-\lambda\dot{\Delta}) - M \exp(-N\sigma)} \tag{4}$$

For purely cohesive soils, $N = 0$ and τ is only a function of Δ and $\dot{\Delta}$. For granular material, $M = A$ and C_d is zero. and τ is a function of Δ and σ. For mixed soils exhibiting shearing resistance due to both frictional and cohesive components, τ is dependent on Δ, $\dot{\Delta}$, and σ. In the following section, the equations of motions for a track-laying vehicle during steering are developed using the proposed soil model (Equation 4) in conjunction with track slippage, centrifugal forces, and vehicle characteristics.

DERIVATION OF TERRAIN-VEHICLE MODEL

Boundary Conditions

The geometry of the vehicle and the boundary conditions of the proposed model are shown schematically in Figure 3. The XYZ coordinates are the local coordinate system of which X is always the longitudinal axis of the vehicle and Y is a transverse axis parallel to the ground. These axes intersect at the center of geometry of the vehicle O. The Z axis is a vertical axis passing through the origin O. The center of gravity of the vehicle (CG) lies on the X axis and is displaced by a distance C_X from the origin. The numerical value of C_X is assumed to be positive if CG is displaced forward from the center of geometry of the vehicle. The XY coordinates of the instantaneous center of rotation ICR are $P + C_X$ and $\tilde{R}$, respectively, where P is the offset. The center of rotation and the radius of the trajectory of the CG are, respectively, CR and R_o. The height of the center of gravity measured from ground surface is denoted by H. The length of the track-ground contact, the track width, and the tread of the tracks are L, D, and B, respectively. As shown in Figure 3, the components of the inertial forces F_C in X and Y directions are, respectively, F_{CX} and F_{CY}. The weight of the vehicle is W.

(11 66)

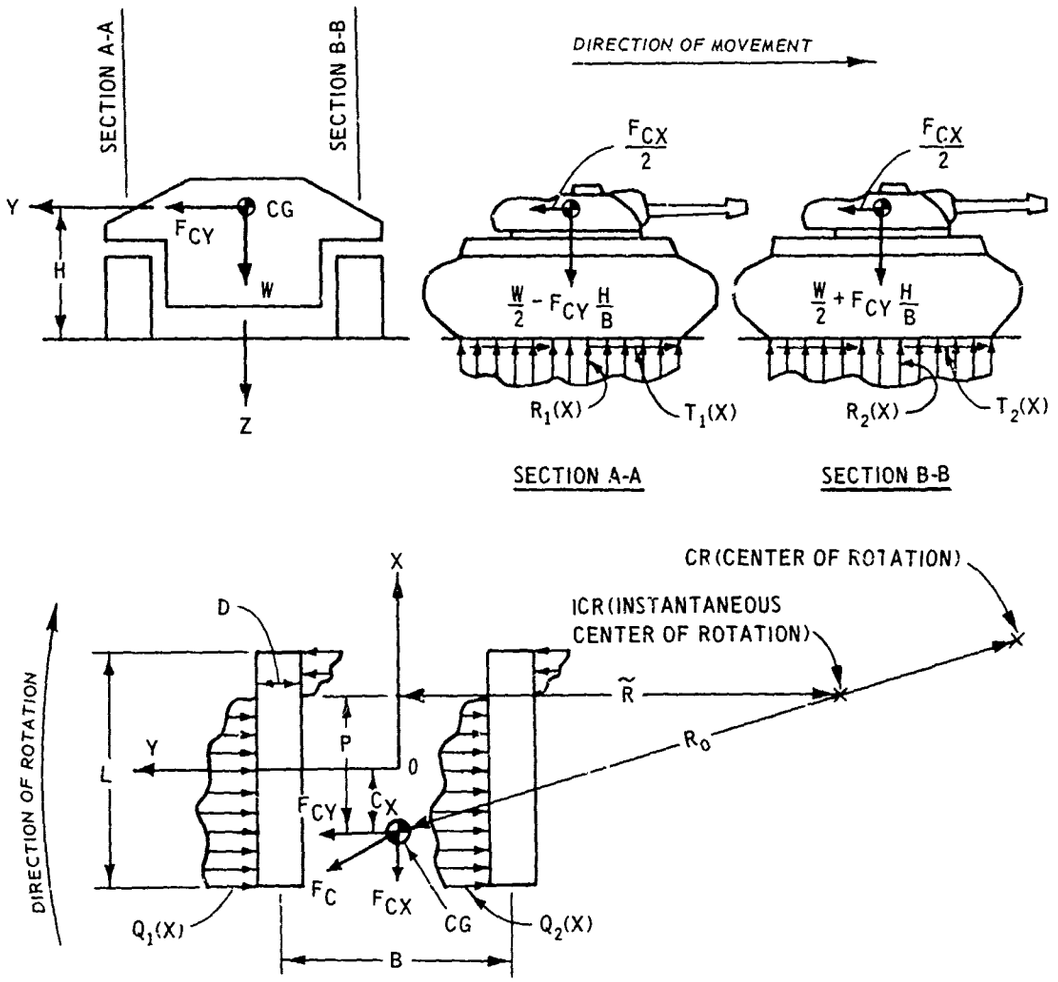

Figure 3. Geometry and boundary conditions of the terrain-vehicle model.

Stress Distribution Along the Tracks

Two types of stress, i.e., normal and shear stresses, exist along the track. As indicated in Figure 3, the normal stresses under the outer and inner tracks are denoted by $R_1(X)$ and $R_2(X)$, respectively. The components of the shear stress in X and Y directions are respectively, $T_1(X)$ and $Q_1(X)$ for the outer track, and $T_2(X)$ and $Q_2(X)$ for the inner track. These stresses are dependent

on the terrain type, vehicle configuration, and speed and turning radius of the vehicle.

The magnitude of normal stresses $R_1(X)$ and $R_2(X)$ can be determined in terms of the components of the inertial force, the track tensions, and the characteristics of the vehicle by considering the balance of vertical stresses and their moments in Figure 3.* Thus:

$$R_1(x) = \frac{W}{dL^2}\left[\frac{1}{2} + 6xc_X - \frac{h}{b}\frac{F_{CY}}{W} - 6hx\frac{F_{CX}}{W}\right] \tag{5}$$

$$R_2(x) = \frac{W}{dL^2}\left[\frac{1}{2} + 6xc_X + \frac{h}{b}\frac{F_{CY}}{W} - 6hx\frac{F_{CX}}{W}\right] \tag{6}$$

where $h = H/L$, $b = B/L$, $d = D/L$, $c_X = C_X/L$, $x = X/L$, $y = Y/L$, and $z = Z/L$.

The components of the shear stress in the X and Y directions along both the outer and inner tracks can be obtained by combining Equations 4, 5, and 6. Thus (it is noted that R_1 and R_2 replace the normal stress σ in Equation 4)

$$T_i(x) = \frac{W}{L^2}\mu\delta_i\left\{\frac{da + dc_d - dc_d\exp(-\lambda\dot{\delta}_i) - m\exp[-nr_i(x)]}{\mu|\delta_i|d+da+dc_d-dc_d\exp(-\lambda\dot{\delta}_i) - m\exp[-nr_i(x)]}\right\}\cos\gamma_1 \tag{7}$$

$$Q_i(x) = \frac{W}{L^2}\mu\delta_i\left\{\frac{da + dc_d - dc_d\exp(-\lambda\dot{\delta}_i) - m\exp[-nr_i(x)]}{\mu|\delta_i|d+da+dc_d-dc_d\exp(-\lambda\dot{\delta}_i) - m\exp[-nr_i(x)]}\right\}\sin\gamma_i \tag{8}$$

where $i = 1,2$; $r_i(x) = 2dL^2R_i(x)/W$; $\delta_i = \Delta_i/L$; $\dot{\delta}_i = \dot{\Delta}_i/L$; $\mu = GL^3/W$; $\lambda = \Lambda L$; $a = AL^2/W$; $m = ML^2/W$; $n = NW/L^2$; and $c_d = C_dL^2/W$. The variables γ_1 and γ_2 , in Equations 7 and 8, are the slip angles and can be written as

$$\left.\begin{aligned}\gamma_1 &= \tan^{-1}\frac{X - P - C_X}{C_1} = \tan^{-1}\frac{x - p - c_X}{\xi_1}\\ \gamma_2 &= \tan^{-1}\frac{X - P - C_X}{C_2} = \tan^{-1}\frac{x - p - c_X}{\xi_2}\end{aligned}\right\} \tag{9}$$

* For sake of brevity, the effect of track tension is not included in this paper. The reader is referred to Reference 7 for a complete analysis of track tension and its effect on steering performance of tracked vehicles.

where $\xi_1 = C_1/L$, $\xi_2 = C_2/L$, and $p = P/L$. The parameter C_1 is the distance between the instantaneous center of rotation of the outer track and its axis of symmetry, and C_2 is the distance between the instantaneous center of rotation of the inner track and its axis of symmetry.

In order to use Equations 7-9, the track slip velocities and displacements (i.e., $\dot{\Delta}_1$, Δ_1 , $\dot{\Delta}_2$, and Δ_2), and the inertial forces F_{CX} and F_{CY} , have to be determined.

Kinematics of the Vehicle

A tracked vehicle in transient motion is shown schematically in Figure 4. The XYZ coordinates are the local coordinate systems that are fixed with respect to the moving vehicle (also see Figure 3). The origin 0 of this coordinate system stays, for all time, at a distance C_X from the center of gravity of the vehicle. The $\Psi\Phi$ coordinate system is fixed on level ground, and its origin coincides with the center of gravity at time zero. The vehicle can maneuver on the $\Psi\Phi$ plane and the displacements of the center of gravity of the vehicle from this reference frame are $\Psi(t)$ and $\Phi(t)$.

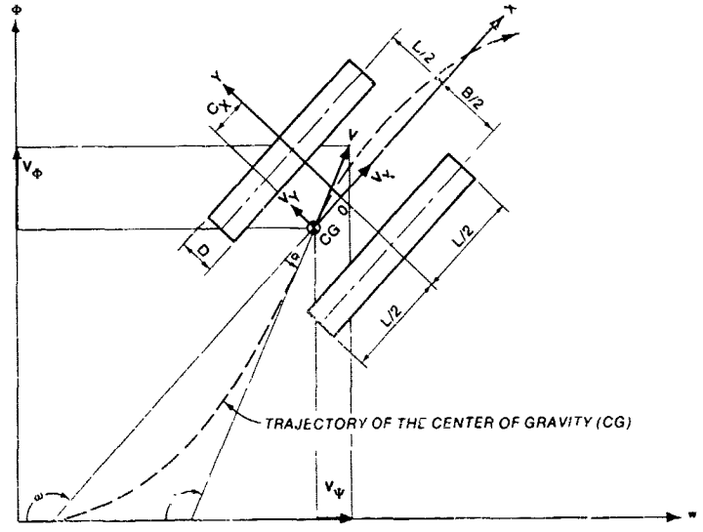

Figure 4. Tracked vehicle in transient motion.

The velocities v_X and v_Y (relative to the origin of the $\Psi\Phi$ coordinate system) as well as the velocities v_Ψ and v_Φ are related to the instantaneous velocity v of the CG by

(169)

$$v = \sqrt{v_X^2 + v_Y^2} = \sqrt{v_\psi^2 + v_\phi^2} \tag{10}$$

The side-slip angle α, which is the angle between the velocity vector v and the longitudinal X axis of the vehicle, is related to the velocities v_X and v_Y as

$$\alpha = \tan^{-1} \frac{v_Y}{v_X} \quad , \quad \frac{d\alpha}{dt} = \left(v_X \frac{dv_Y}{dt} - v_Y \frac{dv_X}{dt} \right) \Big/ v^2 \tag{11}$$

The yaw angle ω and the directional angle Θ are related to α as

$$\Theta = \omega - \alpha \ , \ \frac{d\Theta}{dt} = \frac{d\omega}{dt} - \frac{d\alpha}{dt} \tag{12}$$

Substitution of Equation 11 into Equation 12 leads to

$$\frac{d\Theta}{dt} = \frac{d\omega}{dt} - \left(v_X \frac{dv_Y}{dt} - v_Y \frac{dv_X}{dt} \right) \Big/ v^2 \tag{13}$$

The radius of curvature of the trajectory of the center of gravity (i.e., the distance between CR and CG, Figure 3) is

$$R_o = v \Big/ \frac{d\Theta}{dt} = \frac{v^3}{v^2 \frac{d\omega}{dt} - v_X \frac{dv_Y}{dt} + v_Y \frac{dv_X}{dt}} \tag{14}$$

The coordinates of the trajectory of the center of gravity of the vehicle can be written as

$$\left.\begin{aligned} \Psi(t) &= -\int_0^t v \cos \Theta \, dt \\ \Phi(t) &= \int_0^t v \sin \Theta \, dt \end{aligned}\right\} \tag{15}$$

The coordinates of the instantaneous center of rotation (ICR) of the hull in the XY systems $(X_I \ , \ Y_I)$ and the instantaneous radius of curvature are (Figure 3)

and

$$\left.\begin{aligned} X_I &= P + C_X = v_Y \Big/ \frac{d\omega}{dt} + C_X \\ Y_I &= \tilde{R} = v_X \frac{d\omega}{dt} \\ R_I &= \sqrt{\tilde{R}^2 + P^2} \end{aligned}\right\} \tag{16}$$

170

Track Slip Velocity and Displacement

Assume that v_{s1} ($v_{s1} = \dot{\Delta}_1$) and v_{s2} ($v_{s2} = \dot{\Delta}_2$) are the slip velocities of geometrically similar points of the outer track and the inner track, respectively. The X and Y components of these velocities can be shown to be

$$\left.\begin{aligned} v_{sX1} &= C_1 \frac{d\omega}{dt} = \xi_1 L \frac{d\omega}{dt} \\ v_{sY1} &= (X - P - C_X) \frac{d\omega}{dt} = L(x - c_X) \frac{d\omega}{dt} - v_Y \end{aligned}\right\} \text{For the outer track} \quad (17)$$

$$\left.\begin{aligned} v_{sX2} &= C_2 \frac{d\omega}{dt} = \xi_2 L \frac{d\omega}{dt} \\ v_{sY2} &= v_{sY1} \end{aligned}\right\} \text{For the inner track} \quad (18)$$

The angular velocity $d\omega/dt$ and $\tilde{R}$ can be written as

$$\left.\begin{aligned} \frac{d\omega}{dt} &= \frac{1}{bL} (v_{X1} - v_{sX1} - v_{X2} + v_{sX2}) \\ \tilde{R} &= \frac{1}{2\frac{d\omega}{dt}} (v_{X1} - v_{sX1} + v_{X2} - v_{sX2}) \end{aligned}\right\} \quad (19)$$

where v_{X1} = the velocity of the outer track in X direction
v_{X2} = the velocity of the inner track in X direction

The ratio of v_{X1} and v_{X2} is defined as the steering ratio ε. Thus,

$$\varepsilon = v_{X1}/v_{X2} \quad (20)$$

Substitution of Equations 16 and 20 into Equation 19 leads to

$$v_{sX1} = \varepsilon v_{X2} - \left(v_X + \frac{bL}{2} \frac{d\omega}{dt}\right) \text{For the outer track} \quad (21)$$

$$v_{sX2} = v_{X2} - \left(v_X - \frac{bL}{2} \frac{d\omega}{dt}\right) \text{For the inner track} \quad (22)$$

Comparison between Equations 21 and 22 and Equations 17 and 18 results in

$$\xi_1 = (\varepsilon v_{X2} - v_X) \Big/ \left(L \frac{d\omega}{dt}\right) - \frac{b}{2} \quad (23)$$

(171)

$$\xi_2 = (v_{X2} - v_X) \Big/ \left(L \frac{d\omega}{dt}\right) + \frac{b}{2} \tag{24}$$

The slip velocities and displacements of the outer and inner tracks can be obtained from Equations 17, 18, 21, and 22. Thus,

$$\frac{v_{s1}}{\sqrt{Lg}} = \sqrt{\frac{L}{g}} \frac{d\omega}{dt} \sqrt{\xi_1^2 + \left[(x - c_X) - \frac{v_Y}{L \frac{d\omega}{dt}}\right]^2} \tag{25}$$

$$\frac{v_{s2}}{\sqrt{Lg}} = \sqrt{\frac{L}{g}} \frac{d\omega}{dt} \sqrt{\xi_2^2 + \left[(x - c_X) - \frac{v_Y}{L \frac{d\omega}{dt}}\right]^2} \tag{26}$$

$$\frac{\Delta_1}{L} = \int_0^{t_1} \frac{v_{s1}}{L} dt + \frac{\Delta_{I1}}{L}, \quad \frac{\Delta_2}{L} = \int_0^{t_2} \frac{v_{s2}}{L} dt + \frac{\Delta_{I2}}{L} \tag{27}$$

where $t_1 = (L/2 - X)/v_{X1}$

$t_2 = (L/2 - X)/v_{X2}$

Δ_{I1} = initial displacement of the outer track

Δ_{I2} = initial displacement of the inner track

The balance of forces and moments dictates that these initial displacements be numerically equal to $L\delta$ (δ is the coefficient of rolling resistance which must be measured experimentally for each soil type and each vehicle).

Inertial Forces

The X and Y components of the inertial force can be shown to be (7).

$$F_{CX} = \frac{W}{g} a_x = \frac{W}{g}\left(\frac{dv_X}{dt} + v_Y \frac{d\omega}{dt}\right), \quad F_{CY} = \frac{W}{g}\left(\frac{dv_Y}{dt} - v_X \frac{d\omega}{dt}\right) \tag{28}$$

The Rolling Resistance

The rolling resistance is a function of terrain type, vehicle speed, track condition, etc. Therefore, rolling resistance should be measured for every specific condition. In this formulation, however, the rolling resistance is assumed to be proportional to normal load. Thus,

172

$$R_s = \frac{W}{dL^2}\,\delta \int_{-\frac{1}{2}}^{\frac{1}{2}} [r_1(x) + r_2(x)]\,dx \tag{29}$$

Equations of Motion

Steerability and stability of tracked vehicles depend on the dynamic balance between all forces and moments applied on the vehicle. According to Figure 4, the following three equations govern the motion of the vehicle:

$$\int_{-\frac{1}{2}}^{\frac{1}{2}} [t_1(x) + t_2(x)]\,dx - \delta \int_{-\frac{1}{2}}^{\frac{1}{2}} [r_1(x) + r_2(x)]\,dx = f_{CX} \tag{30}$$

$$\int_{-\frac{1}{2}}^{\frac{1}{2}} [q_1(x) + q_2(x)]\,dx = f_{CY} \tag{31}$$

$$\int_{-\frac{1}{2}}^{\frac{1}{2}} [q_1(x) + q_2(x)](x - c_X)\,dx + \frac{b}{2} \int_{-\frac{1}{2}}^{\frac{1}{2}} [t_1(x) - t_2(x)]\,dx + \frac{b}{2}\,\delta \int_{-\frac{1}{2}}^{\frac{1}{2}} [r_2(x) - r_1(x)]\,dx = \frac{I_z}{LW}\frac{d^2\omega}{dt^2} \tag{32}$$

where $t_1(x) = dL^2\, T_1(x)/W$, $t_2(x) = dL^2\, T_2(x)/W$, $q_1(x) = dL^2\, Q_1(x)/W$, $q_2(x) = dL^2\, Q_2(x)/W$, $f_{CX} = F_{CX}/W$, and $f_{CY} = F_{CY}/W$

and I_z = mass moment of inertia about an axis passing through the center of gravity of the vehicle and parallel to the Z axis (Figure 3). Equations 30 through 32 with the aid of Equations 7 through 29 constitute three equations that involve three unknowns. The three unknowns are either v_X, v_Y, and $d\omega/dt$ or ξ_1, ξ_2, and p. In order to obtain a complete solution for either of the two sets of unknowns, one of the following driving conditions must be specified:

(173)

(a) time history of the steering ratio $\varepsilon(t)$ and the initial speed of the vehicle, (b) time history of the velocity of the individual tracks $v_{X1}(t)$ and $v_{X2}(t)$ and the initial speed of the vehicle, (c) time history of the velocity of the vehicle $v(t)$ and the trajectory of motion, (d) time history of the velocity of the vehicle and a constant value of steering ratio ε, or (e) the trajectory of motion and a determination of the maximum velocity time history at which the vehicle can traverse the specified trajectory. A computer program called AGIL was developed to solve Equations 30 through 32 using Newton's iteration technique. In addition, this computer program has the capability of calculating the power requirements at the sprockets (7).

Correlation with Test Results

In order to determine the accuracy and range of application of the terrain-vehicle model, a series of steering tests was conducted on several different terrains with various soil strengths in the vicinity of Vicksburg, Mississippi. The tracked vehicle used for these experiments is an armored personnel vehicle with characteristics: $W = 18{,}000$ lb , $L = 105$ in. , $H_2 = 35.7$ in. , $D = 15$ in. , $B = 90$ in. , $I_z = 92{,}000$ lb-in.-sec^2 and $C_x = 0$. Each experiment involved steering the vehicle in a circular path, by first accelerating the vehicle to a maximum speed (controlled by either the available power or the stability conditions of the vehicle) and then continue turning with a more or less constant speed. Data collected during each test consisted of time histories of (a) the inner and outer track velocities, (b) the speed of the vehicle, (c) the turning radius, and (d) the power requirement. In addition, for each terrain several in situ direct shear tests were conducted to characterize the soil and to determine the parameters of the soil model. The results of these steering tests are presently being analyzed for correlation and comparison with the terrain-vehicle model predictions. The result of one of the tests which was recently analyzed and correlated with model prediction is presented in this paper. This particular test was conducted on a soft clay soil with characteristics: $G = 200$ psi/in. , $A = 5$ psi , $M = 4.06$ psi , $N = 0.22$ 1/psi , $C_d = 0.61$ psi , and $\Lambda = 3.68$ sec/in. The coefficient of rolling resistance for the vehicle was measured experimentally and has a value $\delta = 0.2$.

To correlate the test data with model predictions, the measured time histories of the inner and outer track velocities were used to drive the model. For these specified driving conditions, the time histories of the vehicle speed and power requirements were then predicted and compared with the corresponding field measurements. Figures 5a and 5b depict the time histories of the inner and outer track

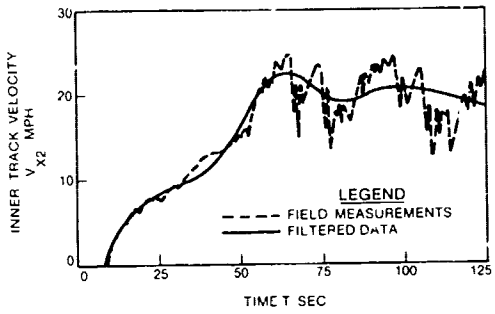

Figure 5a. Inner track velocity-time history.

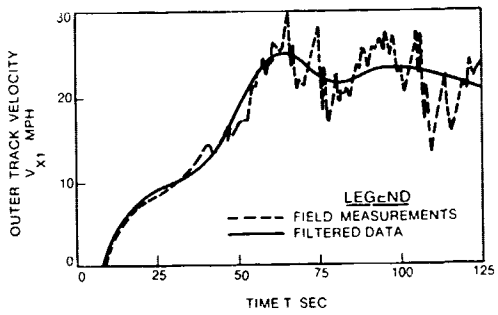

Figure 5b. Outer track velocity-time history.

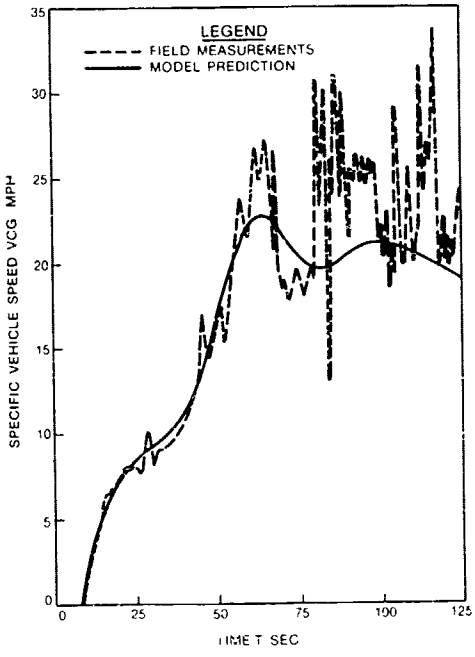

Figure 5c. Vehicle velocity-time history, field measurement versus model prediction.

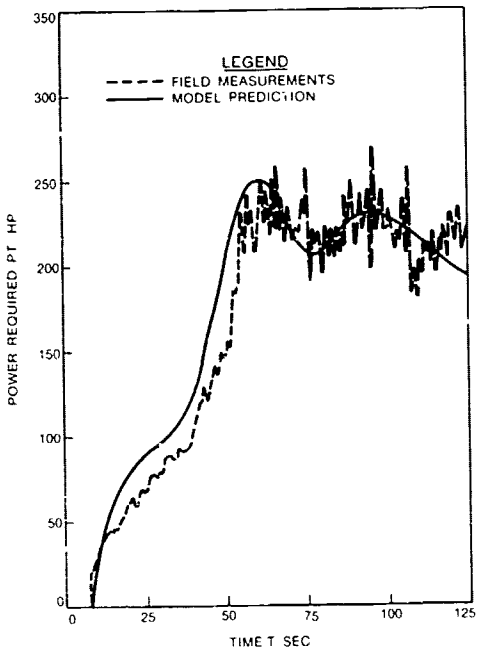

Figure 5d. Total power-time history, field measurement versus model prediction.

175

velocities, respectively. As observed from these figures, the actual field measurements are quite noisy during the steady state portion of the steering (i.e., for times greater than approximately 60 sec). These high frequency oscillations are believed to be mostly due to instrumentation and must be filtered out. The filtered records are also shown in Figures 5a and 5b and are simply "best" fit curves to the field measurements satisfying the condition that the total area under both curves should be equal. These filtered track velocity-time histories were used as input to drive the terrain-vehicle model.

Comparisons of the predicted time histories of the vehicle speed and power requirements during steering with the corresponding field measurements are shown in Figures 5c and 5d. Similar to Figures 5a and 5b, the field measurements are quite noisy during the steady state steering. The predicted results, of course, do not manifest these oscillations because of the filtering of the input data. The degree of correlation of the predicted and measured results, however, is quite good, indicating that the modeling of the overall interaction between the soil and the track is physically reasonable.

ACKNOWLEDGEMENT

The work reported herein was conducted at the U.S Army Engineer Waterways Experiment Station under the sponsorship of the Office, Chief of Engineers, Department of the Army, as part of Project 4A161102AT24, "Effect of Terrain and Climate on Army Material."

The authors are grateful to Mr. Clifford J. Nuttall, Jr., for providing valuable insight during the course of this study, and acknowledge the efforts of Mr. Donald E. Barnes for assisting in the numerical calculations.

REFERENCES

1. Bekker, M. B. 1963. The Theory of Land Locomotion, The University of Michigan Press, Ann Arbor, Mich.

2. Hayashi, I. 1975. "Practical Analysis of Tracked Vehicle Steering Depending on Longitudinal Track Slippage," Proceedings, The International Society for Terrain Vehicle Systems Conference, Vol 2, p 493.

3. Kitano, M. and Jyorzaki, H. 1976. "A Theoretical Analysis of Steerability of Tracked Vehicles," Journal of Terramechanics, The International Society for Terrain Vehicle Systems, Vol 13, No. 4, pp 241-258.

(176)

4. Kitano, M. and Kuma, M. 1977. "An Analysis of Horizontal Plane Motion of Tracked Vehicles," Journal of Terramechanics, The International Society for Terrain Vehicle Systems, Vol 14, No. 4, pp 221-225.

5. Baladi, G. Y. and Rohani, B. 1978. "A Mathematical Model of Terrain-Vehicle Interaction for Predicting the Steering Performance of Track-Laying Vehicles," Proceedings of the 6th International Conference of the International Society for Terrain-Vehicle Systems, Vienna, Austria.

6. Kondner, R. L. "Hyperbolic Stress-Strain Response: Cohesive Soils," Journal, Soil Mechanics and Foundations Division, American Society of Civil Engineers, Vol 89, No. SM1, Feb 1963, pp 115-143.

7. Baladi, G. Y. and Rohani, B. 1979. "A Terrain-Vehicle Interaction Model for Analysis of Steering Performance of Track-Laying Vehicles," Technical Report GL-79-6, U.S. Army Engineer Waterways Experiment Station, CE, Vicksburg, Miss.